All-optical switching in a photonic crystal with a defect containing an N-type four-level atomic system

V. G. Arkhipkin* and S. A. Myslivets†
L. V. Kirensky Institute of Physics, SB RAS, Krasnoyarsk, Russia
(Received 27 September 2012; published 17 December 2012)

We study the transmission spectra of a one-dimensional photonic crystal with a defect containing a four-level atomic medium that exhibits a greatly enhanced third-order susceptibility while having a vanishing linear susceptibility dependent on the electromagnetically induced transparency. Two ways of controlling the transmission of a photonic crystal are discussed: via absorption, i.e., nonlinear (two-photon) absorption of the probe field enhanced by constructive quantum interference, and via dispersion, which comes down to shifting the resonance frequency of the defect mode for the probe field by varying the refractive index based on the giant Kerr nonlinearity (cross-phase modulation). We demonstrate that such systems enable nonlinear all-optical switching at ultralow intensities of the coupling and switching laser fields.

DOI: 10.1103/PhysRevA.86.063816 PACS number(s): 42.50.Gy, 42.70.Qs, 42.25.Hz, 37.10.Jk

I. INTRODUCTION

Linear and nonlinear optical properties of an atomic medium can be controlled by means of coherence and quantum interference [1,2] effects induced by resonant laser fields, which lead to a variety of interesting phenomena for fundamental research and practical applications. Much attention has been paid to electromagnetically induced transparency (EIT) and its effect on the linear and nonlinear susceptibilities of optical media [3–7]. Due to the vanishing linear absorption, significant reduction of group velocity, and enhancement of nonlinear polarizability in an EIT medium, nonlinear optics can be studied at low light levels [3,4,6,7]. To this end, quantum systems are used having various level configurations such as Λ and double-Λ schemes [3], tripod schemes [8], Y- [9] and N-type schemes [10], and others. In four-level systems, EIT can be controlled using additional laser radiation [6,7]. For media with an N-type configuration of levels under EIT (Fig. 1), turning on a third field (switching) of frequency ω_3 can induce nonlinear absorption of the probe field at ω_1 [6] and cross-Kerr nonlinearity, referred to as giant Kerr nonlinearity [7]. Experimental studies of these effects have been reported in quite a few papers [11–15].

EIT combined with a photonic crystal (PC) provides a new tool for manipulating light and achieving a complex functionality due to their unique properties [16]. From that point of view, PCs with micro- and nanodefects, otherwise called micro- and nanocavities [17], are of a particular interest. Structures like that have recently attracted much attention due to their ability to strongly confine light for long times in a very tiny spatial region [18]. This enables the initially low-energy laser radiation to interact even with single atoms [19]. It has been shown that in PCs with a defect containing an EIT medium, the defect-mode Q factor for the probe radiation can greatly increase, whereas the width of the transmission spectrum narrows [20–22]. An all-optical switch has been suggested in [23] based on a PC microcavity with a giant Kerr nonlinearity. Switching occurs due to the shift of the transmission band (defect mode) under applied additional external laser radiation. Such photonic crystal structures are of great interest for integration of various optical functions and fundamental studies in optical physics. For example, they can be used to miniaturize controlled optical filters, for high-precision sensors and atomic clocks, as well as for all-optical switching, and quantum memory in EIT.

This paper reports a theoretical study of the optical properties of a multilayer PC with a defect containing an N-shaped four-level system (Fig. 1), where additional laser radiation of frequency ω_3 (the switching field) is used to effectively control the EIT in order to modify the spectral characteristics of the PC. Due to the effect of light localization in the defect, the intensity of the switching field entering the PC can be very low. Two mechanisms of controlling the probe light pulses passing through the PC are considered: an absorptive mechanism, i.e., due to nonlinear absorption of the probe field, and a dispersive mechanism that comes down to the shifting of the resonance frequency of the defect mode for the probe field resulting from the change of the refractive index owing to the giant Kerr nonlinearity. Spatial nonuniformity of the interacting fields is taken into consideration, unlike the cases of [20,23]. It is shown that in the first case the energy of the switching field can be lower than in the case of the dispersive mechanism, and can correspond to that of single photons (even of one single photon) in the pulse.

The paper is organized as follows. In Sec. II we discuss the susceptibility of a four-level N-type medium at the probe wave frequency in the presence of two strong fields. In Sec. III we present the results of computation of the spectral properties of a one-dimensional photonic crystal with a defect containing an N-type atomic medium. Section IV concludes the paper.

II. SUSCEPTIBILITY OF A FOUR-LEVEL N-TYPE MEDIUM TO THE PROBE WAVE

An energy level diagram of the N-type four-level atomic system is shown in Fig. 1. The level $|0\rangle$ is the ground state and $|2\rangle$ is a metastable state. Initially, only the ground state is populated while all the other levels are not. Transitions $|0\rangle$-$|1\rangle$, $|1\rangle$-$|2\rangle$, and $|2\rangle$-$|3\rangle$ are allowed, and the $|0\rangle$-$|2\rangle$ transition is

*vga@iph.krasn.ru
†sam@iph.krasn.ru

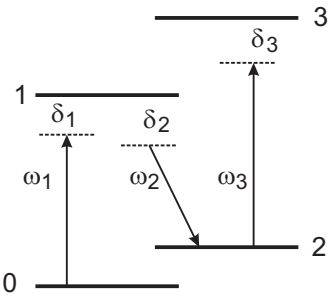

FIG. 1. Energy-level diagram of an N-type four-level atom interacting with a weak probe field (ω_1) and two strong fields: the coupling (ω_2) and the switching (ω_3) fields. $\delta_{1,2,3}$ denote the frequency detuning from one-photon resonances for the probe, coupling, and switching fields, respectively.

dipole forbidden. A resonant coupling laser of frequency ω_2 and amplitude E_2 driving the transition $|1\rangle$-$|2\rangle$ and a weaker probe beam of frequency ω_1 and amplitude E_1 driving the transition $|0\rangle$-$|1\rangle$ create standard Λ-type EIT. A switching laser of frequency ω_3 and amplitude E_3 drives the $|2\rangle$-$|3\rangle$ transition. We take all the fields to be monochromatic and $|E_1| \ll |E_{2,3}|$, and assume that the atoms remain in the ground state for the whole time.

The absorption and refractive indices for the probe field are determined by the imaginary and the real parts of the macroscopic susceptibility $\chi(\omega_1)$. The latter can be calculated from the density matrix equations by finding an exact solution for the strong fields and a first-order perturbation theory solution for the probe field (see, e.g., [5,6]):

$$\chi(\omega_1) = i\chi_0 \frac{\gamma_{10}}{2} \frac{\Delta_{20}\Delta_{30} + |\Omega_3|^2}{\Delta_{10}\Delta_{20}\Delta_{30} + \Delta_{10}|\Omega_3|^2 + \Delta_{30}|\Omega_2|^2}, \quad (1)$$

where $\Delta_{10} = \gamma_{10}/2 - i\delta_1$, $\Delta_{20} = \gamma_{20}/2 - i(\delta_1 - \delta_2)$, $\Delta_{30} = \gamma_{30}/2 - i(\delta_1 - \delta_2 + \delta_3)$, $\delta_1 = \omega_1 - \omega_{10}$, $\delta_2 = \omega_2 - \omega_{12}$, and $\delta_3 = \omega_3 - \omega_{32}$ are the frequency detunings; ω_{ij} and γ_{ij} are the frequencies and widths of the respective transitions; $2\Omega_k = d_{ij}E_k/\hbar$ is the Rabi frequency; E_k ($k = 1,2,3$) is the field amplitude; d_{ij} are the matrix elements of electric dipole moments of transitions; $\chi_0 = |d_{01}|^2 N/\hbar\gamma_{10} = \chi_{0m}N$, where χ_{0m} is the resonant microscopic susceptibility; and N is the atomic concentration.

When $\Omega_3 = 0$ (the switching field is off) the susceptibility (1) takes the form

$$\chi(\omega_1) = i\frac{\chi_0}{2} \frac{\Delta_{20}\gamma_{10}}{\Delta_{20}\Delta_{10} + |\Omega_2|^2}. \quad (2)$$

Formula (2) describes an EIT phenomenon [3] which occurs due to interference of quantum transitions under a strong coupling field. The destructive interference results in an inhibited resonance (one-photon) absorption and a high dispersion of the refractive index for the probe field. The effect is observed under a two-photon (Raman) resonance $\delta_1 - \delta_2 = 0$ and $|\Omega_2|^2 \gg \gamma_{10}\gamma_{20}/4$ [1]. One of the most important consequences of EIT is the reduced group velocity of the probe pulse (slow light) [3].

The spectral dependences Im χ and Re χ normalized to the linear resonance susceptibility χ_0 are shown in Fig. 2 for various Rabi frequencies of the switching field Ω_3 and frequency detuning δ_3. With $\Omega_3 = 0$ (the switching field is off), there is a transparency window in the center due to EIT [Fig. 2(a)]. Once a third field is on, an additional resonance (peak) is observed in the center of the window [Figs. 2(a) and 2(b)]. As the switching field power increases, the central peak becomes higher, while the side peaks become lower and undergo a shift. Note that the smaller is γ_{30}, the lower is the intensity of the switching field at which the central peak is observed.

The existence of three resonances can be explained in terms of "quasilevels" determined as follows [1,5]. The denominator in (1), $D = \Delta_{10}\Delta_{20}\Delta_{30} + \Delta_{10}|\Omega_3|^2 + \Delta_{30}|\Omega_2|^2$, is a cubic polynomial over δ_1. Applying a factorization $D = (\delta_1 - z_1)(\delta_1 - z_2)(\delta_1 - z_3)$, where z_i ($i = 1,2,3$) are the roots of the cubic equation $D = 0$, and making a decomposition to simple fractions, the susceptibility (1) can be cast into a very convenient form for interpretation [5]:

$$\chi(\omega_1) = i\chi_0 \frac{\gamma_{10}}{2} \frac{(\Delta_{20}\Delta_{30} + \Omega_3|^2)}{(z_1 - z_2)} \left[\frac{(z_1 - z_3)^{-1}}{\delta_1 - z_1} - \frac{(z_2 - z_3)^{-1}}{\delta_1 - z_2} + \frac{(z_2 - z_3)^{-1} - (z_1 - z_3)^{-1}}{\delta_1 - z_3} \right]. \quad (3)$$

The parameters z_i are called quasilevels. They determine the position and the width of new resonances. Expression (3) suggests that in the general case there can be three resonances, and the susceptibility has the nature of an interference [3,5,24]. In every particular case the interference pattern depends on the intensity of the coupling and the switching fields, frequency detunings, and relaxation parameters. The position and the number of resonances, as can be seen, depend on the relation between the Rabi frequency of the switching field and its detuning δ_3. Note that the central peak [Fig. 2(a)] corresponds to the case when $\delta_1 = \delta_2 = \delta_3 = 0$, i.e., all the three fields are on resonance.

Figures 2(c) and 2(d) illustrate the Re χ dependences on the normalized probe field detuning under different conditions. One can see that the Re χ behavior is also strongly dependent on the Rabi frequency Ω_3 and the detuning δ_3.

For the sake of better understanding the physics behind the spectral dependencies of Im $\chi(\omega_1)$ and Re $\chi(\omega_1)$, consider the case of a weak switching field $|\delta_3| \gg |\Omega_3|, \gamma_{30}$. In this case, the susceptibility (1) takes the form

$$\chi(\omega_1) = \chi_1^{(1)}(\omega_1) + \chi_{33}^{(3)}(-\omega_1, \omega_3, -\omega_3, \omega_1)|E_3|^2, \quad (4)$$

where $\chi_1^{(1)}(\omega_1)$ is the linear susceptibility of the medium for the probe responsible for EIT; $\chi_{33}^{(3)}$ is the nonlinear third-order susceptibility, the real part of which is called the Kerr susceptibility (to be more exact, the cross-Kerr susceptibility). Note that Re $\chi_{33}^{(3)}$ leads to the effect of cross-phase modulation of the refractive index for the probe radiation.

When $\delta_1 = \delta_2 = 0$, $|\Omega_2|^2 \gg \gamma_{10}\gamma_{20}/4$, the susceptibilities in (4) take the simple forms

$$\chi_1^{(1)}(\omega_1) = i\chi_0 \frac{\gamma_{10}\gamma_{20}}{4|\Omega_2|^2}, \quad (5)$$

$$\chi_{33}^{(3)}(\omega_1) = \frac{|d_{01}|^2|d_{23}|^2 N}{8\hbar^3} \frac{1}{|\Omega_2|^2} \left(i\frac{\gamma_{30}}{2\delta_3^2} - \frac{1}{\delta_3} \right). \quad (6)$$

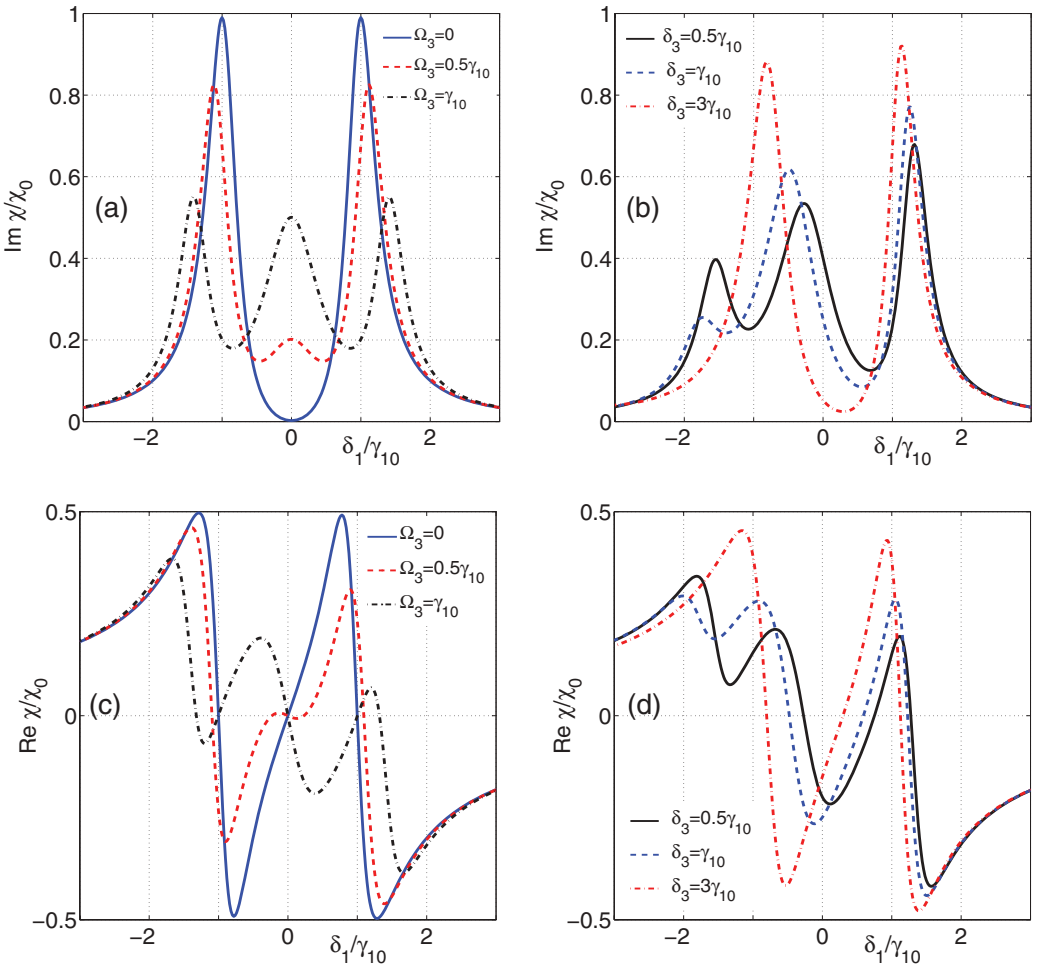

FIG. 2. (Color online) The dispersive behavior of the imaginary (a),(b) and real (c),(d) parts of the nonlinear susceptibility $\chi(\omega_1)$ as the probe frequency detuning varies. $\Omega_2 = \gamma_{10}$, $\delta_2 = 0$, $\gamma_{10} = \gamma_{30} = 2\pi \times 10$ MHz, $\gamma_{20} = 0.01\gamma_{10}$. (a),(c) $\delta_3 = 0$. (b),(d) $\Omega_3 = \gamma_{10}$.

From (5) and (6) one can see that $\chi_1^{(1)}$ is purely imaginary due to the exact two-photon resonance, and $\mathrm{Im}\,\chi_1^{(1)}/\chi_0 \ll 1$, and it is $\chi_{33}^{(3)}$ that gives a nonlinear contribution to the absorption and the refractive index of the probe wave. So, when there is no third field, virtually no absorption of the probe radiation occurs owing to EIT [Fig. 2(a), solid line]. The switching on of Ω_3 results in a nonlinear absorption of the probe field (dashed and dash-dotted lines) because $\mathrm{Im}\,\chi(\omega_1) = \mathrm{Im}(\chi_{33}^{(3)})|E_3|^2 \gg \mathrm{Im}\,\chi_1^{(1)}$. Using (6), it can be shown that the magnitude of this absorption can be comparable to the linear absorption in a two-level system and $\mathrm{Re}\,\chi_{33}^{(3)}$ can be many orders of magnitude higher than the Kerr susceptibility in a conventional three-level cascade scheme with a two-photon resonance (under similar conditions) [10]. Therefore $\mathrm{Re}\,\chi_{33}^{(3)}$ is referred to as the giant Kerr susceptibility.

In the dressed-state basis $|+\rangle = (|1\rangle + |2\rangle)/\sqrt{2}$ and $|-\rangle = (|1\rangle - |2\rangle)/\sqrt{2}$, the nonlinear absorption of the probe field can be interpreted as absorption of two photons $\hbar\omega_1$ and $\hbar\omega_3$ (two-photon absorption) enhanced by constructive quantum interference [3,6,7,25]. In this case, one-photon absorption is inhibited by EIT.

The giant Kerr nonlinearity and nonlinear absorption have been studied experimentally in hot and cold atoms as well as in Bose condensates [11–15]. The feasibility of all-optical switching of the probe radiation by using a weak switching field (tens to hundreds of photons per switching pulse) has been demonstrated. We note that this scheme allows the group velocity of the probe pulse to be controlled in the range from $v_g \ll c$ to $v_g < 0$ [26].

In what follows, we will discuss the effect of absorptive and Kerr nonlinearities on the spectral properties of a one-dimensional PC with a defect containing N-type atomic systems.

III. SPECTRAL PROPERTIES OF PC WITH A DEFECT CONTAINING AN N-TYPE ATOMIC MEDIUM

A. The model and basic approximations

Let us consider a one-dimensional PC with the structure $(\mathrm{HL})^M\mathrm{HDH}(\mathrm{LH})^M$. Here H and L refer to dielectric layers with high (H) and low (L) refractive indices n_H and n_L, and the widths d_H and d_L; the structure period is $t = d_\mathrm{H} + d_\mathrm{L}$; M is the number of bilayers (periods); D is the defect layer with the refractive index n_D and the width d. The defect layer is

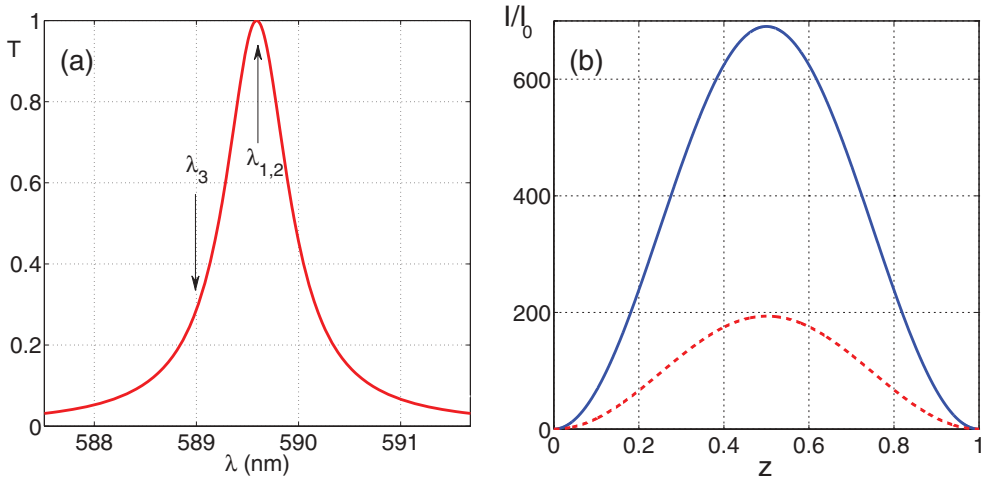

FIG. 3. (Color online) (a) PC defect mode without an EIT medium. The arrows indicate the positions of the interacting wavelengths. (b) Spatial distribution of the intensity I/I_0 of the coupling (solid curve) and switching (dashed curve) fields in the defect layer as functions of the normalized (to the layer width d_D) coordinate z; $z = 0$ and $z = 1$ correspond to the defect boundaries; I_0 is the input intensity.

filled with a medium comprised of four-level N-type atoms, which we will assume to be immobile and noninteracting with each other. Initially, only the lowest state $|0\rangle$ is populated.

Three plane monochromatic waves of frequencies $\omega_{1,2,3}$ and amplitudes $E_{1,2,3}$ are normally incident on the PC and propagate along the z axis from left to right. We will proceed on the assumption that the probe field amplitude (E_1) in the defect layer is much smaller than the amplitudes of the driving (E_2) and switching (E_3) fields. Within this approximation, the refractive index for the probe field inside the defect in the presence of two strong fields can be defined as

$$n_D = n = 1 + i2\pi\chi_0 \frac{\gamma_{10}}{2} \frac{\Delta_{20}\Delta_{30} + |\Omega_3|^2}{\Delta_{10}\Delta_{20}\Delta_{30} + \Delta_{10}|\Omega_3|^2 + \Delta_{30}|\Omega_2|^2}. \quad (7)$$

For the numerical simulation, we used parameters typical of the D lines of a sodium atom. The probe wavelength corresponds to the transition around the D_1 line $\lambda = 589.6$ nm, and the levels $|0\rangle$ and $|2\rangle$ correspond to superfine splitting at the transition frequency $\omega_{21} = 2\pi \times 1.8$ GHz. We will assume the refractive indices for the coupling and switching fields to be equal to unity in the defect.

Any individual field ($i = 1,2,3$) in the j layer (j corresponds to the layers H, L, and D) can be treated as a superposition of the direct (incident) and returning (reflected) waves:

$$E_{i,j}(z) = A_{i,j}(z)\exp(iq_{i,j}z) + B_{i,j}(z)\exp(-iq_{i,j}z), \quad (8)$$

where $A_{i,j}$ and $B_{i,j}$ are the amplitudes of the direct and returning waves; $q_{i,j} = k_i n_{i,j}$, $k_i = 2\pi/\lambda_i$, and $n_{i,j}$ is the refractive index for the ith wave in the jth layer. The amplitudes of the direct and the returning waves can be found from the appropriate wave equations by applying the recurrence relations technique [27–29]. The transmission (T) and the reflection (R) coefficients for the probe wave are determined by

$$T = |A_{1L}|^2/|A_{10}|^2, \quad R = |B_{10}|^2/|A_{10}|^2. \quad (9)$$

Here A_{10} and A_{1L} are the input and output amplitudes of the probe wave and B_{10} is the amplitude of the probe wave reflected from the entrance face of the PC.

The transmission spectra of the probe wave have been calculated for various Rabi frequencies of the switching field for a PC having the following parameters: $M = 5$, $n_H d_H = n_L d_L = \lambda_0/4$, $n_D d_D = \lambda_0/2$, $n_H = 2.35$, and $n_L = 1.45$. Here the wavelength $\lambda_0 = 589.6$ nm corresponds to the center of the band gap of the PC. The optical width of the defect layer $d_D n_D$ is chosen such that for the indicated parameters the defect mode occurs in the center of the band gap and its spectral width is broad enough for all three waves to fall within this transmission band. Figure 3(a) shows the transmission spectrum of the PC for the probe field in the absence of an EIT medium ($n_D = 1$) in the defect layer. The arrows show the positions of all the field frequencies with respect to the defect mode. Figure 3(b) shows the spatial distribution of the coupling (solid curve) and switching (dashed curve) intensity $I(z)$ scaled to the input intensity I_0 in the PC. One can see that the fields are localized in the defect layer. Because of the closeness of the frequencies ω_1 and ω_2, the spatial distribution of the probe field virtually coincides with that of the coupling field.

B. Use of nonlinear absorption to modify the transmission spectrum of the PC

Let us first consider the feasibility of modifying spectral properties of PCs due to nonlinear absorption when the coupling and the switching fields are on resonance, i.e., $\delta_2 = \delta_3 = 0$. The PC parameters have been chosen such that the $|1\rangle$-$|0\rangle$ transition frequency coincides with the defect-mode resonance frequency.

The transmission of a PC strongly depends on the absorption and dispersive properties of the medium placed in the defect. As the field in the defect is enhanced owing to localization, a lower input intensity can be used than in a conventional cell. Since the space distribution of the fields in the defect is nonuniform, the Rabi frequencies of the driving

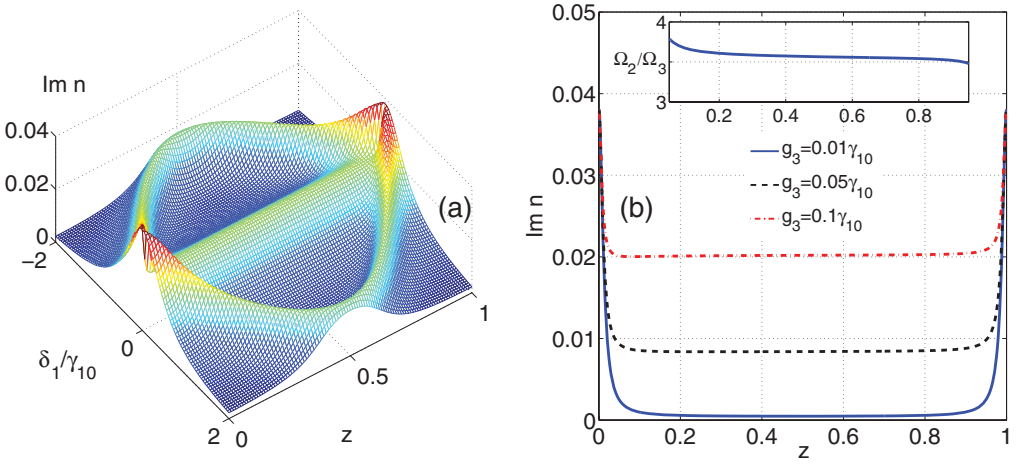

FIG. 4. (Color online) (a) Im n dependence on the probe field detuning and the normalized coordinate z in the defect layer for $g_3 = 0.1\gamma_{10}$. (b) Im n distribution inside the defect layer under resonance conditions $\delta_1 = 0$ for various g_3 values. $g_2 = 0.05\gamma_{10}$, $\gamma_{10} = \gamma_{30} = 2\pi \times 10$ MHz, $\gamma_{20} = 0.01\gamma_{10}$, $\chi_0 = 8.4 \times 10^{-3}$.

and the switching fields depend on the spatial coordinate z: $\Omega_{2,3} = \Omega_{2,3}(z)$. Hence the refractive index for the probe wave is also a function of the z coordinate. Below we will use Ω for the Rabi frequency inside the defect and g for the Rabi frequency when entering the PC: $\Omega(z) = gF(z)$, where $F(z) = I(z)/I_0$.

Figure 4(a) shows the typical dependence Im n as a function of the probe detuning and the coordinate z in the defect layer for given values of the Rabi frequencies $g_{2,3}$ when entering the PC. In most of the defect a splitting into three resonances is observed. The largest splitting takes place in the center of the defect, where the fields reach their maximum. Near the boundaries of the defect, where the coupling and switching fields are close to zero, there is no splitting. Here, Im n is determined by the linear absorption. As will be shown below, the linear absorption zones, although rather small, produce a noticeable effect on the PC transmission.

Note that nonlinear absorption [the central peak in Fig. 4(a)] is virtually the same over the entire length of the defect even though the fields are distributed nonuniformly. This unusual behavior can be explained as follows. With the use of Eq. (7) it can be shown that under resonance conditions and for $|\Omega_2|^2 \gg \gamma_{10}\gamma_{20}/4$ and $|\Omega_3|^2 \gg \gamma_{30}\gamma_{20}/4$, the expression for Im n takes the form

$$\mathrm{Im}\, n \sim \frac{\gamma_{10}}{\gamma_{10} + \gamma_{30}|\Omega_2(z)|^2/|\Omega_3(z)|^2}. \qquad (10)$$

From Eq. (10) it is seen that Im $n(z)$ depends on the relation between the Rabi frequencies of the coupling and switching fields. The $|\Omega_2(z)|^2/|\Omega_3(z)|^2$ ratio varies insignificantly over most of the defect, as can be seen in the inset in Fig. 4(b).

Figure 5 shows the PC transmission spectra for the probe field at various input Rabi frequencies g_3. In the absence of the coupling and the switching fields, there is a deep dip in the center (the solid curve in the inset in Fig. 5) associated with resonance absorption at the $|0\rangle$-$|1\rangle$ transition (see, e.g., [28] and references therein). With the coupling field on and $g_3 = 0$, a narrow resonance is observed in the transmission curve (the dashed curve in the inset in Fig. 5), which is attributed to EIT [20,21]. Switching on a third field reduces transmission because of the absorption, the mechanism of which was discussed above. By varying the power of the switching field, the transmission of the PC can be modified as shown in Fig. 5

Figure 6 shows the probe field transmission coefficient as a function of the Rabi frequency g_3 of the switching field entering the PC under resonance conditions $\delta_1 = \delta_2 = \delta_3 = 0$. The initial concentration of atoms is chosen such that the transmission of the probe radiation is close to zero in the absence of the coupling field. With the coupling field on, maximum transmission is observed due to EIT. When the switching field is turned on, the transmission is reduced by induced nonlinear absorption. The transmission decreases with increasing g_3.

Let us estimate the input intensity I_3 of the switching field required to reduce the PC transmission to half the value for the case corresponding to the solid curve in Fig. 6. From the figure, we can see that it approximately corresponds to $g_3 = 0.012\gamma_{10}$. For the input intensity we find $I_3 = 3.6\ \mu\mathrm{W/cm}^2$, whereas the

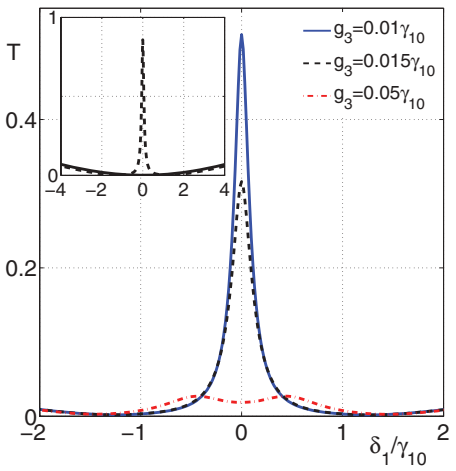

FIG. 5. (Color online) PC transition spectra for various Rabi frequencies of the switching field g_3. The rest of the parameters are as in Fig. 4. The inset shows transmission spectra for $\Omega_{2,3} = 0$ (solid curve) and for $g_3 = 0$ under EIT (dashed curve).

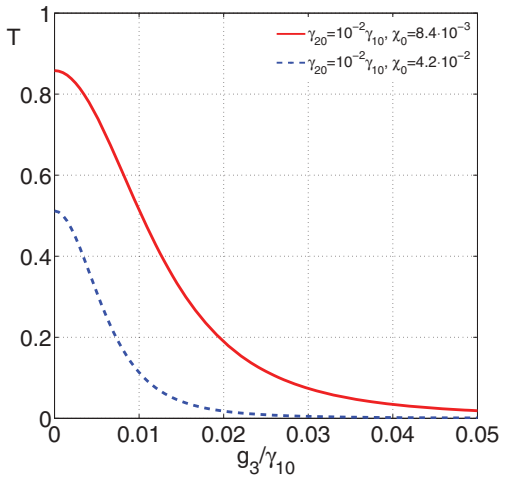

FIG. 6. (Color online) Transmission coefficient of the probe field versus the Rabi frequency of the switching field: $g_2 = 0.05\gamma_{10}$, $\gamma_{10} = \gamma_{30} = 2\pi \times 10$ MHz.

driving field intensity required for EIT, $g_2 = 0.05\gamma_{10}$ is $I_2 = 60\ \mu\mathrm{W/cm}^2$. These intensities, as indicated by the estimates, correspond to single photons in a 10 μs pulse per the area λ^2.

C. Use of giant Kerr nonlinearity to modify PC transmission

Let us discuss the effect of the dispersive part of the refractive index (7) on the PC transmission spectrum. As shown above in Sec. II, turning on an off-resonant switching field generates a nonlinear (Kerr) contribution to the refractive index, which can be large enough to shift the defect mode in the spectrum and to reduce transmission of the probe wave. Figure 7(a) shows the transmission spectrum for the case of Kerr (dispersive) nonlinearity in the defect layer as a function of the input Rabi frequency g_3 of the switching field at the fixed detuning $\delta_3 = 30\gamma_{30}$. The transmission spectra corresponding to $g_3 = 0$ (dotted curve) and $g_3 = 0.42\gamma_{10}$ (dash-dotted curve) are given in Fig. 7(b). It can be seen that as the amplitude of the switching field grows, the transmission peak shifts and gets wider and smaller. The shift of the transmission spectrum is associated with the change in the refractive index while the transmission attenuation occurs due to linear resonance absorption near the boundaries of the defect (the EIT has disappeared) and residual nonlinear off-resonant absorption of the probe field. The contribution from the latter, as indicated by calculations, appears to be significant.

In our case, the drop in the transmission maximum is much more pronounced than in [23] because such factors as nonuniform spatial distribution of the coupling and switching fields and nonlinear off-resonant absorption of the probe field have been taken into account. Note that in [23] it was assumed that a single atom was placed in the center of the defect, and the detuning was chosen to be $\delta_3 \gg \gamma_{30}$, so the nonlinear off-resonance absorption of the probe field was neglected. The solid curve [Fig. 7(b)] shows the transmission of the PC with uniform spatial distribution of the fields. The dashed curve corresponds to a hypothetical case when spatial nonuniformity of the coupling and switching fields and the nonlinear off-resonance absorption are ignored ($\gamma_{30} = 0$).

In order to achieve switching, the transmission band has to be shifted by a magnitude larger than the transmission bandwidth. However, in this case a higher intensity will be required for switching compared to the case of nonlinear resonance absorption.

D. Probe pulse propagation

We now assume the weak probe field to be a Gaussian pulse $E_1(t) = E_0 \exp(-t^2/\tau_p^2)\exp(i\omega_1 t)$, where E_0 is the amplitude, $2\tau_p = T_p$ is the pulse length at the $\exp(-1)$ level, and ω_1 is the central (carrier) frequency. The coupling and the switching fields are continuous monochromatic waves. The spectrum of the input probe pulse is a Fourier transform of the given pulse:

$$E_{1i}(\omega) = 2^{-1/2}\tau_p E_0 \exp\left[-\tau_p^2(\omega-\omega_1)^2/4\right]. \qquad (11)$$

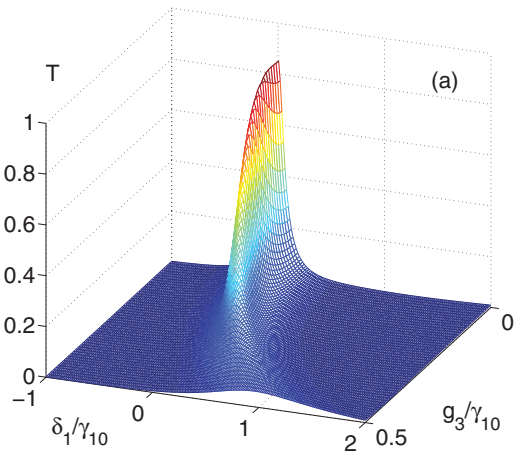

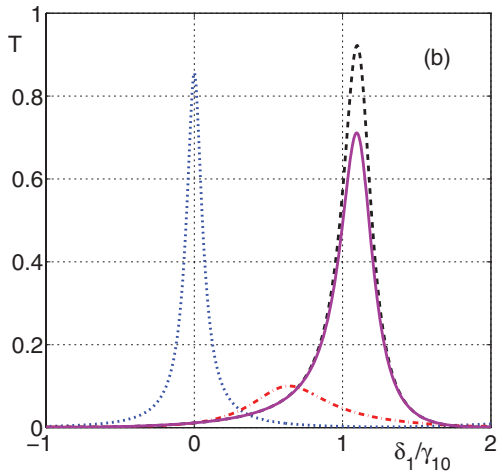

FIG. 7. (Color online) (a) PC transmission spectrum as a function of the probe field frequency detuning and Rabi frequency of the switching field for a fixed detuning $\delta_3 = 30\gamma_{10}$; $g_2 = 0.05\gamma_{10}$, $\gamma_{10} = \gamma_{30} = 2\pi \times 10$ MHz; (b) Fragments of the transmission spectrum for $g_3 = 0$ (dotted curve), $g_3 = 0.42\gamma_{10}$ (dash-dotted curve). The solid curve shows the transmission of PC with uniform spatial distribution of the fields. The dashed curve refers to a hypothetical case when spatial non-uniformity of the fields is ignored and $\gamma_{30} = 0$.

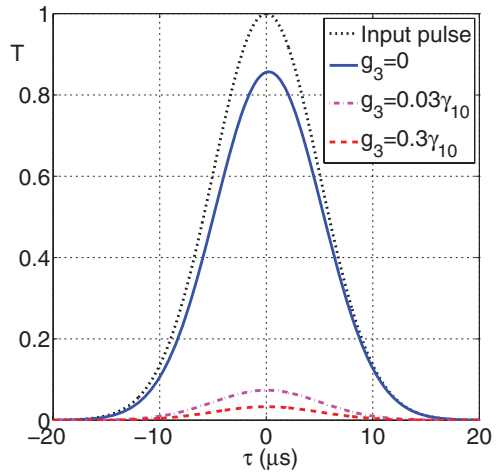

FIG. 8. (Color online) Time dependence of the probe filed pulse. The dotted curve is the input pulse with the pulse length $T_p = 10\,\mu$s. The solid curve is the transmitted pulse under EIT with no switching field. The dash-dot curve refers to the output pulse in the presence of a resonant switching field. The dashed curve refers to the transmitted pulse under off resonant switching field. $g_2 = 0.05\gamma_{10}$.

Knowing the transmission coefficient $T(\omega)$, one can calculate the spectrum of the past pulse:

$$E_t(\omega) = T(\omega)E_{1i}(\omega) = 2^{-1/2}\tau_p E_0 T(\omega)\exp\left[-\tau_p^2(\omega-\omega_1)^2/4\right]. \quad (12)$$

Applying a reverse Fourier transformation, for the output pulse intensity we obtain

$$I_t(t) \propto \left|\frac{1}{\sqrt{2\pi}}\int_{-\infty}^{\infty} E_t(\omega)\exp(-i\omega t)d\,\omega\right|^2. \quad (13)$$

In this approach, the duration of the probe pulse should satisfy the condition $T_p\gamma_{20} \gg 1$ [30].

In Fig. 8 the input and output probe pulses calculated with Eq. (13) are shown as a time function under various conditions. The dotted curve refers to the pulse entering the PC. In the case of an empty defect, the output pulse is virtually identical to the input one. The solid curve refers to the output pulse under EIT in the absence of the switching field. Applying the switching field reduces the output pulse amplitude: the higher the intensity of the switching field, the smaller the amplitude of the output pulse. The dashed curve refers to the output pulse with Kerr nonlinearity in the defect.

IV. CONCLUSION

We have studied theoretically the transmission spectra of a one-dimensional PC with the defect containing an N-type four-level medium under controlled EIT. Two mechanisms underlying the PC transmission control have been studied: absorptive (nonlinear absorption) and dispersive (giant Kerr nonlinearity). A structure like that can function as an all-optical switch of light pulses at ultralow intensities of the coupling and the switching fields. Without a switching pulse, a high transmission of the probe radiation is observed due to EIT. When the switching field is turned on, the transmission is reduced because of the above-mentioned effects. It has been shown that the lowest switching laser power can correspond to one photon and single photons of the coupling pulse. The switch size can be considerably smaller than in a conventional cell. Since nonlinear absorption depends on a simultaneous arrival of the probe and the switching pulses, it may be used to process quantum entangled states [6]. Note that other configurations of atomic levels can be used to control PC transmission [31,32], where microwave or radio frequency fields would act as the switching field. The use of heterostructure semiconductors as nonlinear media with controlled EIT is of great interest [33].

ACKNOWLEDGMENTS

This work was supported in part by the RAS Grants No. 24.29, No. 24.31, and No. 3.9.5, and SB RAS Grants No. 43 and No. 101.

[1] S. G. Rautian, G. I. Smirnov, and A. M. Shalagin, *Nonlinear Resonances in Atomic and Molecular Spectra* (Nauka, Novosibirsk, 1979).
[2] M. O. Scully and M. S. Zubairy, *Quantum Optics* (Cambridge University Press, Cambridge, 1997).
[3] M. Fleischhauer, A. Imamoglu, and J. P. Marangos, Rev. Mod. Phys. **77**, 633 (2005).
[4] S. E. Harris and L. V. Hau, Phys. Rev. Lett. **82**, 4611 (1999).
[5] V. G. Arkhipkin, Quantum Electron. **27**, 341 (1997).
[6] S. E. Harris and Y. Yamamoto, Phys. Rev. Lett. **81**, 3611 (1998).
[7] H. Schmidt and A. Imamoglu, Opt. Lett. **21**, 1936 (1996).
[8] S. Li, X. Yang, X. Cao, C. Xie, and H. Wang, J. Phys. B **40**, 3211 (2007).
[9] Y. Zhang, A. W. Brown, and M. Xiao, Phys. Rev. Lett. **99**, 123603 (2007).
[10] Y. Chen, X. G. Wei, and B. S. Ham, J. Phys. B **42**, 065506 (2009).
[11] M. Yan, E. G. Rickey, and Y. Zhu, Phys. Rev. A **64**, 041801 (2001).
[12] D. A. Braje, V. Balić, G. Y. Yin, and S. E. Harris, Phys. Rev. A **68**, 041801 (2003).
[13] H. Kang and Y. Zhu, Phys. Rev. Lett. **91**, 093601 (2003).
[14] Y.-F. Chen, Z.-H. Tsai, Y.-C. Liu, and I. A. Yu, Opt. Lett. **30**, 3207 (2005).
[15] H.-Y. Lo, Y.-C. Chen, P.-C. Su, H.-C. Chen, J.-X. Chen, Y.-C. Chen, I. A. Yu, and Y.-F. Chen, Phys. Rev. A **83**, 041804 (2011).
[16] M. Soljacic and J. D. Joannopoulos, Nat. Mater. **3**, 211 (2004).
[17] K. J. Vahala, Nature (London) **424**, 839 (2003).
[18] P. Lalanne, C. Sauvan, and J. Hugonin, Laser Photon. Rev. **2**, 514 (2008).

[19] J. Vučković and Y. Yamamoto, Appl. Phys. Lett. **82**, 2374 (2003).
[20] M. Soljacic, E. Lidorikis, L. V. Hau, and J. D. Joannopoulos, Phys. Rev. E **71**, 026602 (2005).
[21] V. G. Arkhipkin and S. A. Myslivets, Quantum Electron. **39**, 157 (2009).
[22] J. Tidström, C. W. Neff, and L. M. Andersson, J. Opt. **12**, 035105 (2010).
[23] M. Soljacic, E. Lidorikis, J. Joannopoulos, and L. Hau, Appl. Phys. Lett. **86**, 171101 (2005).
[24] T. Y. Abi-Salloum, B. Henry, J. P. Davis, and F. A. Narducci, Phys. Rev. A **82**, 013834 (2010).
[25] N. Mulchan, D. G. Ducreay, R. Pina, M. Yan, and Y. Zhu, J. Opt. Soc. Am. B **17**, 820 (2000).
[26] H. Kang, G. Hernandez, and Y. Zhu, Phys. Rev. A **70**, 011801 (2004).
[27] A. V. Balakin, V. A. Bushuev, B. I. Mantsyzov, I. A. Ozheredov, E. V. Petrov, A. P. Shkurinov, P. Masselin, and G. Mouret, Phys. Rev. E **63**, 046609 (2001).
[28] V. G. Arkhipkin, S. A. Myslivets, I. V. Timofeev, A. V. Shabanov, S. Y. Vetrov, and V. P. Timofeev, in *LFNM 2006: Proceedings of the Eighth International Conference on Laser and Fiber-Optical Networks Modeling, Kharkiv, Ukraine*, edited by I. A. Sukhoivanov (IEEE, New York, 2006), pp. 313–316.
[29] V. G. Arkhipkin, V. A. Gunyakov, S. A. Myslivets, V. P. Gerasimov, V. Y. Zyryanov, S. Y. Vetrov, and V. F. Shabanov, JETP **106**, 388 (2008).
[30] M. G. Payne and L. Deng, Phys. Rev. A **64**, 031802 (2001).
[31] S. N. Sandhya and K. K. Sharma, Phys. Rev. A **55**, 2155 (1997).
[32] Y. Niu, S. Gong, R. Li, Z. Xu, and X. Liang, Opt. Lett. **30**, 3371 (2005).
[33] X.-M. Su and J.-Y. Gao, Phys. Lett. A **264**, 346 (2000).